Chapter 6
Spatial Parallel Robotic Machines with Revolute Actuators

6.1 Preamble

In this chapter, first, a six degrees of freedom fully parallel robotic machine with revolute actuators is presented and analyzed. Then, a serial of parallel manipulators with 3-dof, 4-dof, and 5-dof whose degree of freedom is dependent on an additional passive leg, this passive leg is connecting the center between the base and the moving platform. Together with the inverse kinematics and velocity equations for both rigid-link and flexible-link mechanisms, a general kinetostatic model is established for the analysis of the structural rigidity and accuracy of this family of mechanisms, case studies for 3-dof, 4-dof, and 5-dof mechanisms are given in detail to illustrate the results.

6.2 Six Degrees of Freedom Parallel Robotic Machine with Revolute Actuators

6.2.1 Geometric Modeling

Figures 6.1 and 6.2 represent a 6-dof parallel mechanism with revolute actuators. This mechanism consists of six actuated legs with identical topology, connecting the fixed base to a moving platform. The kinematic chains consist – from base to platform – of an actuated revolute joint, a moving link, a Hooke joint, a second moving link, and a spherical joint attached to the platform. A fixed reference frame $O - xyz$ is connected to the base of the mechanism and a moving coordinate frame $P - x'y'z'$ is connected to the platform.

D. Zhang, *Parallel Robotic Machine Tools*, DOI 10.1007/978-1-4419-1117-9_6,

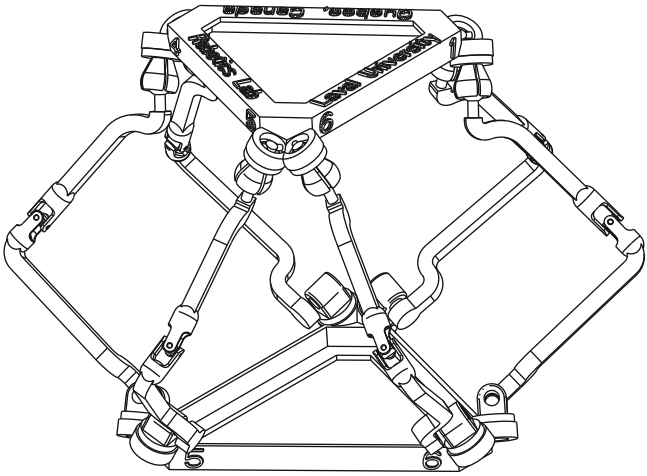

Fig. 6.1 CAD model of the spatial 6-dof parallel mechanism with revolute actuators (Figure by Thierry Laliberté and Gabriel Coté)

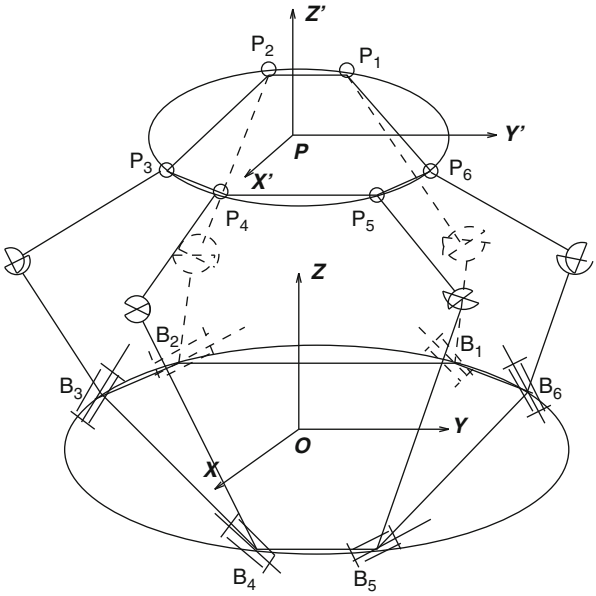

Fig. 6.2 Schematic representation of the spatial 6-dof parallel mechanism with revolute actuators

6.2.2 Global Velocity Equation

6.2.2.1 Rigid Model

The global velocity equation for rigid model can be expressed as

$$\mathbf{At} = \mathbf{B}\dot{\theta}, \tag{6.1}$$

where vectors $\dot{\theta}$ and $\mathbf{t}$ are defined as

$$\dot{\theta} = \left[\, \dot{\theta}_1 \cdots \dot{\theta}_6 \,\right]^{\mathrm{T}}, \tag{6.2}$$

$$\mathbf{t} = \left[\, \omega^{\mathrm{T}},\, \dot{\mathbf{p}}^{\mathrm{T}} \,\right]^{\mathrm{T}} \tag{6.3}$$

and

$$\mathbf{A} = \left[\, \mathbf{m}_1\ \mathbf{m}_2\ \mathbf{m}_3\ \mathbf{m}_4\ \mathbf{m}_5\ \mathbf{m}_6 \,\right]^{\mathrm{T}} \tag{6.4}$$

$$\begin{aligned}\mathbf{B} = \mathrm{diag}[&(\mathbf{p}_1 - \mathbf{b}'_1)^{\mathrm{T}}\mathbf{e}_1, (\mathbf{p}_2 - \mathbf{b}'_2)^{\mathrm{T}}\mathbf{e}_2, (\mathbf{p}_3 - \mathbf{b}'_3)^{\mathrm{T}}\mathbf{e}_3,\\ &(\mathbf{p}_4 - \mathbf{b}'_4)^{\mathrm{T}}\mathbf{e}_4, (\mathbf{p}_5 - \mathbf{b}'_5)^{\mathrm{T}}\mathbf{e}_5, (\mathbf{p}_6 - \mathbf{b}'_6)^{T}\mathbf{e}_6]\end{aligned} \tag{6.5}$$

and $\mathbf{m}_i$ is a six-dimensional vector expressed as

$$\mathbf{m}_i = \begin{bmatrix} (\mathbf{Q}\mathbf{r}'_i) \times (\mathbf{p}_i - \mathbf{b}'_i) \\ (\mathbf{p}_i - \mathbf{b}'_i) \end{bmatrix}, \quad i = 1, \ldots, 6 \tag{6.6}$$

and again, the Jacobian matrix $\mathbf{J}$ can be written as

$$\mathbf{J} = \mathbf{B}^{-1}\mathbf{A}. \tag{6.7}$$

6.2.2.2 Compliant Model

For the case of compliant model, one can obtain the global velocity equation as

$$\mathbf{At} = \mathbf{B}\dot{\theta}, \tag{6.8}$$

where vector $\dot{\theta}$ is defined as

$$\dot{\theta} = \left[\, \dot{\theta}_{11}\ \dot{\theta}_{12}\ \dot{\theta}_{21}\ \dot{\theta}_{22}\ \dot{\theta}_{31}\ \dot{\theta}_{32}\ \dot{\theta}_{41}\ \dot{\theta}_{42}\ \dot{\theta}_{51}\ \dot{\theta}_{52}\ \dot{\theta}_{61}\ \dot{\theta}_{62} \,\right]^{\mathrm{T}} \tag{6.9}$$

matrix $\mathbf{A}$ and its terms are as given in (6.4) and (6.6) and

$$\mathbf{B}_{6\times 12} = \begin{bmatrix} b_{11} & b_{12} & 0 & 0 & 0 & 0 & 0 & 0 & 0 & 0 & 0 & 0 \\ 0 & 0 & b_{21} & b_{22} & 0 & 0 & 0 & 0 & 0 & 0 & 0 & 0 \\ 0 & 0 & 0 & 0 & b_{31} & b_{32} & 0 & 0 & 0 & 0 & 0 & 0 \\ 0 & 0 & 0 & 0 & 0 & 0 & b_{41} & b_{42} & 0 & 0 & 0 & 0 \\ 0 & 0 & 0 & 0 & 0 & 0 & 0 & 0 & b_{51} & b_{52} & 0 & 0 \\ 0 & 0 & 0 & 0 & 0 & 0 & 0 & 0 & 0 & 0 & b_{61} & b_{62} \end{bmatrix}, \quad (6.10)$$

where

$$b_{ij} = (\mathbf{p}_i - \mathbf{b}'_i)^{\mathrm{T}}\mathbf{d}_{ij}, \quad i = 1, \ldots, 6, \ j = 1, 2 \quad (6.11)$$

The derivation of the relationship between Cartesian velocities and joint rates is thereby completed.

6.2.3 Stiffness Model

Again, the stiffness of the structure has been obtained as

$$\mathbf{K} = \mathbf{J}^{\mathrm{T}}\mathbf{K}_{\mathrm{J}}\mathbf{J}. \quad (6.12)$$

One obtains

$$\mathbf{t} = \mathbf{J}'\dot{\theta}, \quad (6.13)$$

where

$$\mathbf{J}' = \mathbf{A}^{-1}\mathbf{B} \quad (6.14)$$

according to the principle of virtual work, one has

$$\tau^{\mathrm{T}}\dot{\theta} = \mathbf{w}^{\mathrm{T}}\mathbf{t}, \quad (6.15)$$

where τ is a vector of the actuator torques applied at each actuated joint or joint with spring. If we assume that no gravitational forces act on any of the intermediate links and $\mathbf{w}$ is a vector composed of forces and moments (hereafter called wrench) applied by the end-effector. Substituting (6.13) into (6.15) one can obtain

$$\tau = \mathbf{J}'^{\mathrm{T}}\mathbf{w}. \quad (6.16)$$

The joint forces and displacements of each joint can be related by Hooke's law, i.e.,

$$\tau = \mathbf{K}_{\mathrm{J}}\Delta\theta. \quad (6.17)$$

$\Delta\theta$ only includes the actuated joints and joint with springs, i.e.,

$$\mathbf{K}_{\mathrm{J}}\Delta\theta = \mathbf{J}'^{\mathrm{T}}\mathbf{w} \quad (6.18)$$

hence

$$\Delta\theta = \mathbf{K}_{\mathrm{J}}^{-1}\mathbf{J}'^{\mathrm{T}}\mathbf{w}. \tag{6.19}$$

premultiplying by $\mathbf{J}'$ on both sides, one obtains

$$\mathbf{J}'\Delta\theta = \mathbf{J}'\mathbf{K}_{\mathrm{J}}^{-1}\mathbf{J}'^{\mathrm{T}}\mathbf{w}. \tag{6.20}$$

Substituting (6.13) into (6.20), one obtains

$$\mathbf{t} = \mathbf{J}'\mathbf{K}_{\mathrm{J}}^{-1}\mathbf{J}'^{\mathrm{T}}\mathbf{w}, \tag{6.21}$$

therefore, one obtains the compliance matrix of the mechanism κ as follow

$$\kappa = \mathbf{J}'\mathbf{K}_{\mathrm{J}}^{-1}\mathbf{J}'^{\mathrm{T}} \tag{6.22}$$

and the system stiffness matrix is

$$\mathbf{K} = [\mathbf{J}'\mathbf{K}_{\mathrm{J}}^{-1}\mathbf{J}'^{\mathrm{T}}]^{-1}, \tag{6.23}$$

where

$$\mathbf{K}_{\mathrm{J}} = \mathrm{diag}[k_{11}, k_{12}, k_{21}, k_{22}, k_{31}, k_{32}, k_{41}, k_{42}, k_{51}, k_{52}, k_{61}, k_{62}] \tag{6.24}$$

where k_{i1} is stiffness of the ith actuator and k_{i2} is the lumped stiffness of each leg.

In order to illustrate the effect of the flexible links on the parallel mechanism, an example of 6-dof mechanism is presented. The parameters are given as

$$\begin{gathered}\theta_{\mathrm{p}} = 22.34°, \theta_{\mathrm{b}} = 42.883°,\\ R_{\mathrm{p}} = 6\,\mathrm{cm}, R_{\mathrm{b}} = 15\,\mathrm{cm},\\ l_{i1} = 46\,\mathrm{cm}, l_{i2} = 36\,\mathrm{cm}, \quad i = 1, \ldots, 6\\ k_{i1} = 1,000\,\mathrm{Nm}, \quad i = 1, \ldots, 6,\end{gathered}$$

where k_{i1} is the stiffness of each leg, l_{i1}, l_{i2} are the link lengths for the 1st and 2nd link of each leg, and the Cartesian coordinates are given by

$$\begin{gathered}x \in [-3, 3]\,\mathrm{cm}, y \in [-3, 3]\,\mathrm{cm}, z = 68\,\mathrm{cm},\\ \phi = 0, \theta = 0, \psi = 0.\end{gathered}$$

Figure 6.3 shows the variation of the stiffness for the above example. The comparison between the parallel mechanism with rigid link and the parallel mechanism with flexible links is given in Table 6.1. The results are similar to those obtained in previous cases.

From Fig. 6.4, one can find that K_x and K_y, K_{θ_x} and K_{θ_y} are symmetric with respect to each other. In Fig. 6.4(a), the stiffness in X becomes higher when the

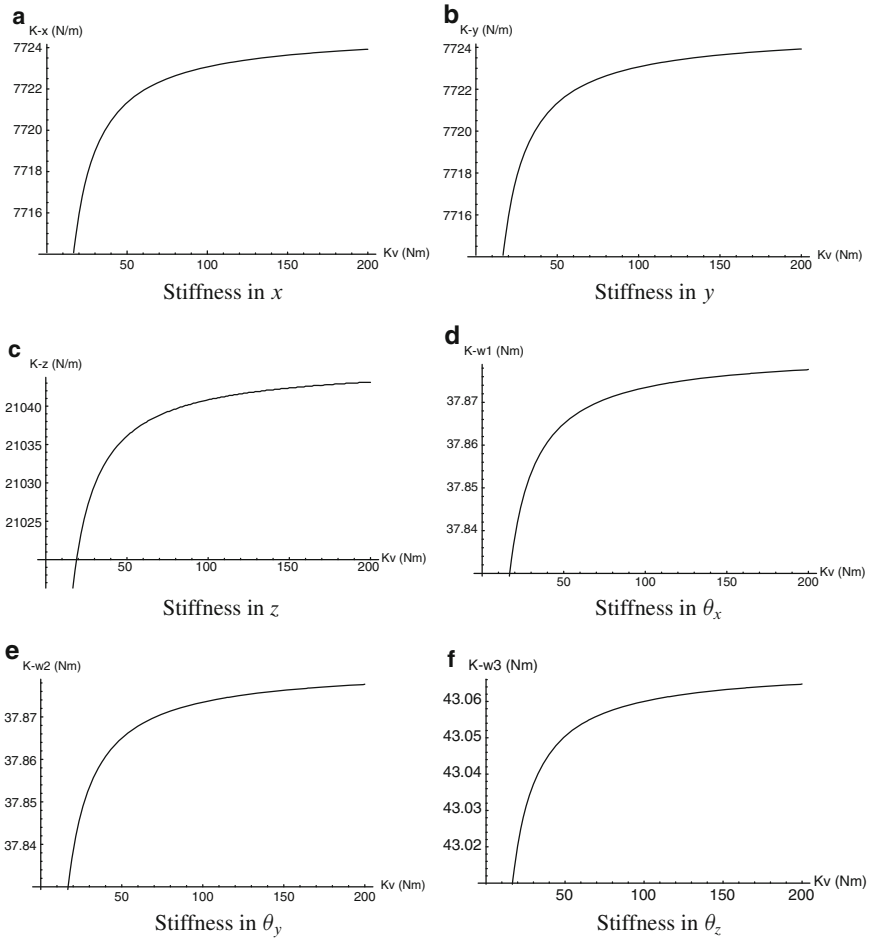

Fig. 6.3 Evolution of the stiffness as a function of the link's lumped stiffness in different directions

Table 6.1 Comparison of the mechanism stiffness between the mechanism with rigid links and the mechanism with flexible links

K_{actuator}	K_{link}	K_x	K_y	K_z	K_{θ_x}	K_{θ_y}	K_{θ_z}
1,000	1,000	3,700.65	3,700.65	10,082.1	18.1478	18.1478	20.633
1,000	$10^1 K_a$	6,967.15	6,967.15	18,981.4	34.1665	34.1665	38.8454
1,000	$10^2 K_a$	7,641.67	7,641.67	20,819.1	37.4743	37.4743	42.6062
1,000	$10^3 K_a$	7,716.37	7,716.37	21,022.6	37.8406	37.8406	43.0227
1,000	$10^4 K_a$	7,723.92	7,723.92	21,043.2	37.8777	37.8777	43.0648
1,000	$10^5 K_a$	7,724.68	7,724.68	21,045.2	37.8814	37.8814	43.069
1,000	$10^6 K_a$	7,724.76	7,724.76	21,045.4	37.8818	37.8818	43.0694
1,000	$10^7 K_a$	7,724.76	7,724.76	21,045.4	37.8818	37.8818	43.0695
1,000	Rigid	7,724.76	7,724.76	21,045.4	37.8818	37.8818	43.0695

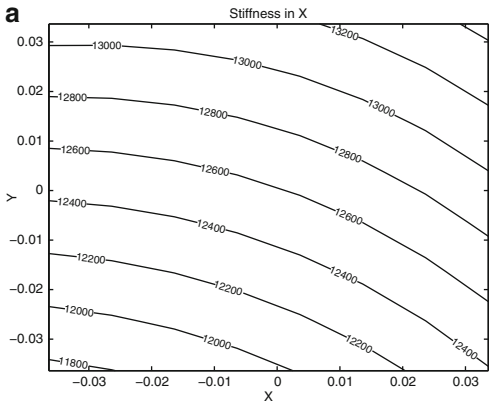

Stiffness in x (N/m)

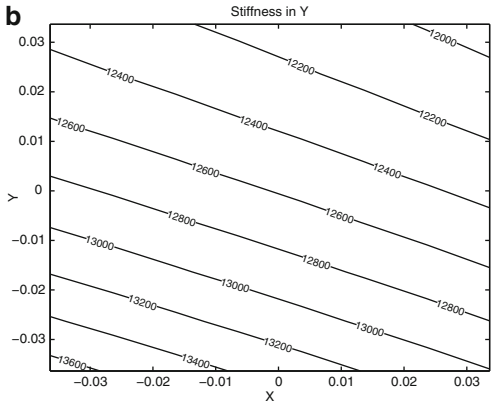

Stiffness in y (N/m)

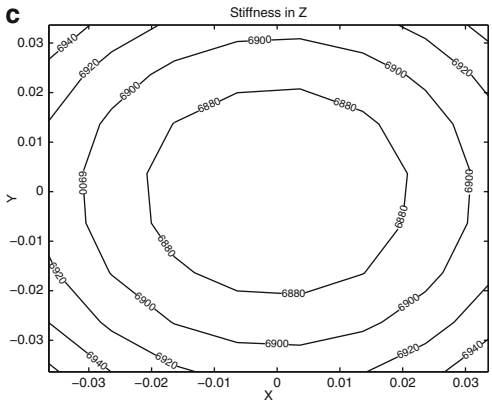

Stiffness in z (N/m)

Fig. 6.4 Stiffness mappings of the spatial 6-dof parallel mechanism with revolute actuators (6 legs) (all length units in m)

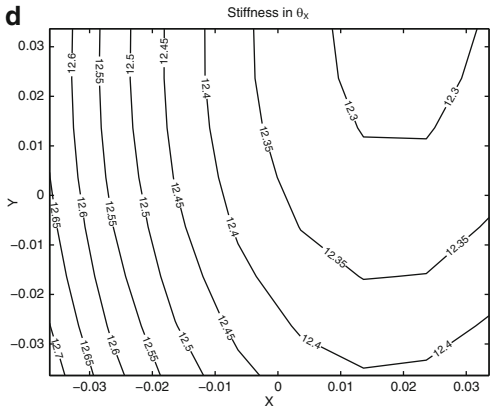

Stiffness in θ_x (Nm)

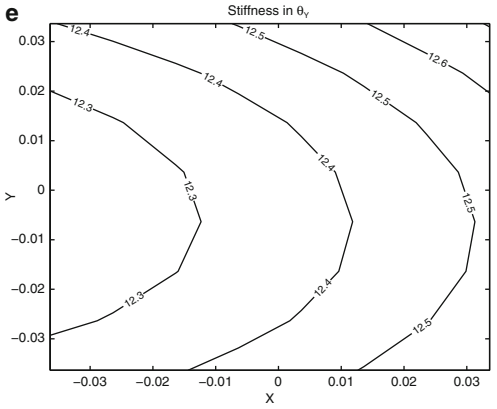

Stiffness in θ_y (Nm)

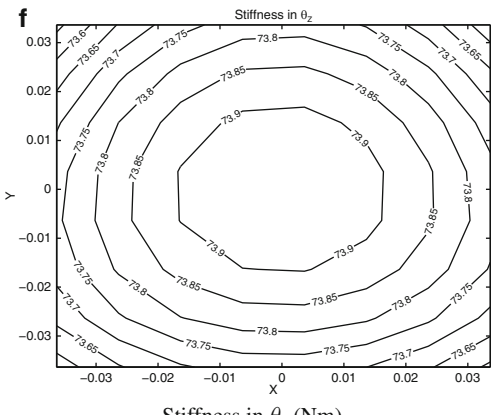

Stiffness in θ_z (Nm)

Fig. 6.4 (continued)

platform moves further from the Y-axis. This was to be expected because when the platform moves aside along the X-axis, the projection of the legs on this axis becomes larger, and the mechanism is stiffer in Y. And the same reasoning applies to Fig. 6.4(b) for the stiffness in Y.

In Fig. 6.4d, e, the torsional stiffnesses in θ_x and θ_y are shown, the stiffness is larger when the platform moves further from the Y-axis. However, in the center of the workspace, the K_z is at its minimum, and the stiffness in the Z becomes higher when the platform moves further from the center of the workspace. On the other hand, from Fig. 6.4(f), the stiffness in θ_z is higher near the center of the workspace, which is the best position for supporting torsional loads around Z-axis. All these are in accordance with what would be intuitively expected.

6.3 General Kinematic Model of *n* Degrees of Freedom Parallel Mechanisms with a Passive Constraining Leg and Revolute Actuators

6.3.1 Geometric Modeling and Lumped Compliance Model

An example of parallel mechanism belonging to the family of mechanisms studied in this chapter is shown in Figs. 6.5 and 6.6. It is a 5-dof parallel mechanism with revolute actuators.

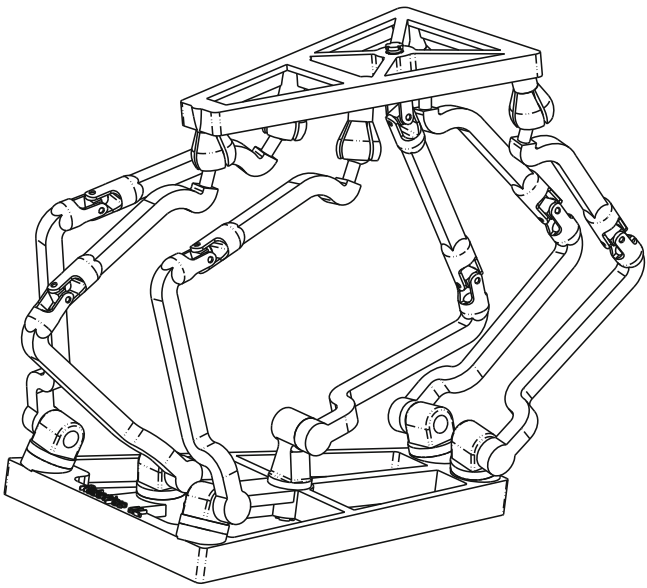

Fig. 6.5 CAD model of the spatial 5-dof parallel mechanism with revolute actuators (Figure by Gabriel Coté)

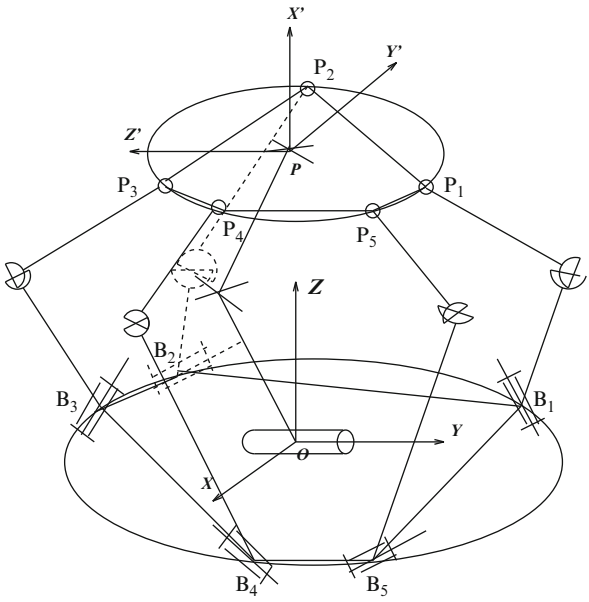

Fig. 6.6 Schematic representation of the spatial 5-dof parallel mechanism with revolute actuators

In order to obtain a simple kinetostatic model, link compliances are lumped at the joints should be considered. In this framework, link bending stiffnesses are replaced by equivalent torsional springs located at virtual joints.

6.3.2 Inverse Kinematics

6.3.2.1 Solution for the Case of Mechanisms with Rigid Links

In order to solve the inverse kinematic problem, one must first consider the passive constraining leg as a serial n-dof mechanism whose n Cartesian coordinates are known, which is a well-known problem. Once the solution to the inverse kinematics of this n-dof serial mechanism is found, the complete pose (position and orientation) of the platform can be determined using the direct kinematic equations for this serial mechanism. Figure 6.7 illustrates the configuration of the ith actuated joint of the mechanism with revolute actuators. Point B_i' is defined as the center of the Hooke joint connecting the two moving links of the ith actuated leg. Moreover, the Cartesian coordinates of point B_i' expressed in the fixed coordinate frame are represented as $(b_{ix}', b_{iy}', b_{iz}')$ and the position vector of point B_i' in the fixed frame is given by vector $\mathbf{b}_i'$. Since the axis of the fixed revolute joint of the ith actuated leg is assumed to be parallel to the xy plane of the fixed coordinate frame, one can write

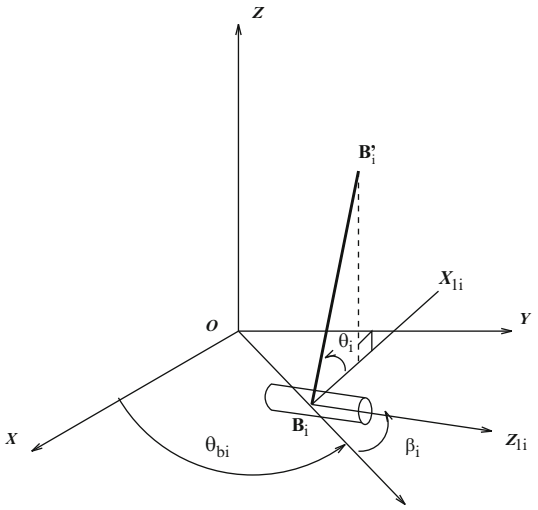

Fig. 6.7 The ith actuated revolute joint

$$b'_{ix} = b_{ix} - l_{i1}\sin(\theta_{bi} + \beta_i)\cos\theta_{i1}, \quad i = 1, \ldots, n, \ n = 3, 4, \text{ or } 5, \tag{6.25}$$

$$b'_{iy} = b_{iy} + l_{i1}\cos(\theta_{bi} + \beta_i)\cos\theta_{i1}, \quad i = 1, \ldots, n, \ n = 3, 4, \text{ or } 5, \tag{6.26}$$

$$b'_{iz} = b_{iz} + l_{i1}\sin\theta_{i1}, \quad i = 1, \ldots, n, \ n = 3, 4, \text{ or } 5, \tag{6.27}$$

where θ_{bi} is the angle between the positive direction of the x-axis of the base coordinate frame and the line connecting points O and B_i and θ_{i1} is the joint variable – rotation angle around the fixed revolute joint – associated with the ith actuated leg, β_i is the angle between the positive direction of the line connecting points O and B_i and the axis of the ith actuated joint. Moreover, l_{i1} is the length of the first link of the ith actuated leg. From the configuration of Fig. 6.7, the relationships between the parameters can be written as

$$(b'_{ix} - x_i)^2 + (b'_{iy} - y_i)^2 + (b'_{iz} - z_i)^2 = l_{i2}^2, \quad i = 1, \ldots, n, \ n = 3, 4, \text{ or } 5, \tag{6.28}$$

where x_i, y_i, z_i are the coordinates of point P_i and l_{i2} is the length of the second link of the ith actuated leg.

Substituting (6.25) – (6.27) into (6.28), one has

$$E_i\cos\theta_{i1} + F_i\sin\theta_{i1} = G_i, \quad i = 1, \ldots, n, \ n = 3, 4, \text{ or } 5, \tag{6.29}$$

where

$$E_i = (y_i - b_{iy})\cos(\theta_{bi} + \beta_i) - (x_i - b_{ix})\sin(\theta_{bi} + \beta_i), \tag{6.30}$$

$$F_i = z_i - b_{iz}, \tag{6.31}$$

$$G_i = \frac{(x_i - b_{ix})^2 + (y_i - b_{iy})^2 + (z_i - b_{iz})^2 + l_{i1}^2 - l_{i2}^2}{2l_{i1}} \tag{6.32}$$

and angle θ_{i1} can be obtained by

$$\sin\theta_{i1} = \frac{F_i G_i + K_i E_i \sqrt{H_i}}{E_i^2 + F_i^2}, \quad i = 1, \ldots, n, \ n = 3, 4, \text{ or } 5, \tag{6.33}$$

$$\cos\theta_{i1} = \frac{E_i G_i - K_i F_i \sqrt{H_i}}{E_i^2 + F_i^2}, \quad i = 1, \ldots, n, \ n = 3, 4, \text{ or } 5, \tag{6.34}$$

where $K_i = \pm 1$ is the branch index of the mechanism associated with the configuration of the ith leg and

$$H_i = E_i^2 + F_i^2 - G_i^2, \quad i = 1, \ldots, n, \ n = 3, 4, \text{ or } 5. \tag{6.35}$$

Finally, the solution of the inverse kinematic problem is completed by performing

$$\theta_{i1} = \text{atan2}[\sin\theta_{i1}, \cos\theta_{i1}], \quad i = 1, \ldots, n, \ n = 3, 4, \text{ or } 5. \tag{6.36}$$

Meanwhile, referring to Fig. 6.7, the vector of leg length can be written as

$$\mathbf{b}_i' = \mathbf{b}_i + l_{i1}\mathbf{Q}_{ti1}\mathbf{d}_i, \quad i = 1, \ldots, n, \ n = 3, 4, \text{ or } 5 \tag{6.37}$$

with

$$\mathbf{Q}_{ti1} = \begin{bmatrix} \cos(\theta_{bi} + \beta_i) & -\sin(\theta_{bi} + \beta_i) & 0 \\ \sin(\theta_{bi} + \beta_i) & \cos(\theta_{bi} + \beta_i) & 0 \\ 0 & 0 & 1 \end{bmatrix}, \quad i = 1, \ldots, n, \ n = 3, 4, \text{ or } 5 \tag{6.38}$$

and

$$\mathbf{d}_{i1} = \begin{bmatrix} 0 \\ \cos\theta_{i1} \\ \sin\theta_{i1} \end{bmatrix}, \quad i = 1, \ldots, n, \ n = 3, 4, \text{ or } 5 \tag{6.39}$$

assuming that the distance between points P_i and B_i' is noted l_{i2}, then one has

$$l_{i2}^2 = (\mathbf{p}_i - \mathbf{b}_i)^{\mathrm{T}}(\mathbf{p}_i - \mathbf{b}_i), \quad i = 1, \ldots, n, \quad n = 3, 4, \text{ or } 5. \tag{6.40}$$

6.3.2.2 Solutions for the Mechanisms with Flexible Links

In order to uniquely describe the architecture of a kinematic chain, i.e., the relative location and orientation of its neighboring pair axes, the Denavit–Hartenberg notation is used to define the nominal geometry of each of the serial kinematic chains of the parallel mechanism. A coordinate frame F_i is defined with the origin O_i and axes X_i, Y_i, Z_i, this frame is attached to the $(i-1)$th link. Figure 6.8 represents one of the identical kinematic chains for the n-dof parallel mechanism discussed above. Joint 2 is a virtual joint used to model the compliance of the driven link.

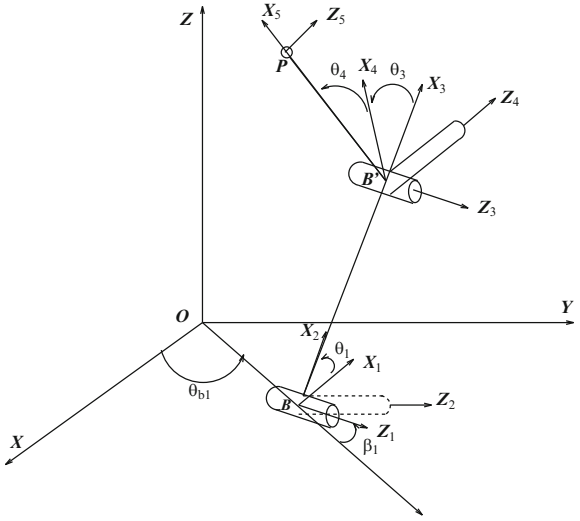

Fig. 6.8 One of the identical kinematic chains with flexible links

From Fig. 6.8, one has $\theta_{i2} = 0$, when there is no deflection. Angles θ_{i3} and θ_{i4} can be obtained by writing the coordinates of point P_i in Frame 3 as

$$x_{i3} = l_{i2}\cos\theta_{i4}\cos\theta_{i3}, \quad i = 1,\ldots,n,\ n = 3, 4, \text{ or } 5, \tag{6.41}$$

$$y_{i3} = l_{i2}\cos\theta_{i4}\sin\theta_{i3}, \quad i = 1,\ldots,n,\ n = 3, 4, \text{ or } 5, \tag{6.42}$$

$$z_{i3} = l_{i2}\sin\theta_{i4}, \quad i = 1,\ldots,n,\ n = 3, 4, \text{ or } 5, \tag{6.43}$$

and

$$[\mathbf{p}]_3 = \mathbf{Q}_{i2}^T\mathbf{Q}_{i1}^T\mathbf{Q}_{i0}^T[\mathbf{p}_i - \mathbf{b}'_i], \quad i = 1,\ldots,n,\ n = 3, 4, \text{ or } 5. \tag{6.44}$$

then, combining (6.41) – (6.43) and (6.44), one can find θ_{i3} and θ_{i4} easily.

From Fig. 6.8, one can express the position of point B'_i as

$$\mathbf{b}'_i = \mathbf{b}_i + \mathbf{Q}_{i0}\mathbf{a}_{i1} + \mathbf{Q}_{i0}\mathbf{Q}_{i1}\mathbf{a}_{i2}, \quad i = 1,\ldots,n,\ n = 3, 4, \text{ or } 5, \tag{6.45}$$

where $\mathbf{Q}_{i0}$, $\mathbf{a}_{i1}$, $\mathbf{a}_{i2}$ and $\mathbf{Q}_{i1}$ can be expressed as

$$\mathbf{a}_{i1} = \begin{bmatrix} 0 \\ 0 \\ 0 \end{bmatrix}, \ \mathbf{a}_{i2} = \begin{bmatrix} l_{i1}\cos\theta_{i2} \\ l_{i1}\sin\theta_{i2} \\ 0 \end{bmatrix}, \ \mathbf{Q}_{i1} = \begin{bmatrix} \cos\theta_{i1} & 0 & \sin\theta_{i1} \\ \sin\theta_{i1} & 0 & -\cos\theta_{i1} \\ 0 & 1 & 0 \end{bmatrix}, \tag{6.46}$$

$$\mathbf{Q}_{i0} = \begin{bmatrix} -\sin(\theta_{bi} + \beta_i) & 0 & \cos(\theta_{bi} + \beta_i) \\ \cos(\theta_{bi} + \beta_i) & 0 & \sin(\theta_{bi} + \beta_i) \\ 0 & 1 & 0 \end{bmatrix}. \tag{6.47}$$

6.3.3 Jacobian Matrices

6.3.3.1 Rigid Mechanisms

The parallel mechanisms studied here comprise two main components, namely, the passive constraining leg – which can be thought of as a serial mechanism – and the actuated legs acting in parallel.

Considering the passive constraining leg, one can write

$$\mathbf{J}_{n+1}\dot{\theta}_{n+1} = \mathbf{t}, \ n = 3, 4, \text{ or } 5, \tag{6.48}$$

where $\mathbf{J}_{n+1}$ consists of $\mathbf{e}_i$ and $\mathbf{r}_i$, $\mathbf{t} = \left[\omega^{\mathrm{T}} \ \dot{\mathbf{p}}^{\mathrm{T}}\right]^{\mathrm{T}}$ is the twist of the platform, ω is the angular velocity of the platform, and $\dot{\theta}_{n+1} = \left[\dot{\theta}_{n+1,1} \cdots \dot{\theta}_{n+1,n}\right]^{\mathrm{T}}$, ($n = 3, 4, \text{ or } 5$) is the joint velocity vector associated with the passive constraining leg. Matrix $\mathbf{J}_{n+1}$ is the Jacobian matrix of the passive constraining leg which is taken as a serial n-dof mechanism.

6.3.3.2 Compliant Model

If the compliances of the links and joints are included, $(6-n)$ virtual joints will then be added to the passive constraining leg in order to account for the compliance of the links [62]. Hence, the Jacobian matrix of the passive constraining leg becomes

$$\mathbf{J}'_{n+1}\dot{\theta}'_{n+1} = \mathbf{t}, \quad n = 3, 4, \text{ or } 5, \tag{6.49}$$

where

$$\dot{\theta}'_{n+1} = \left[\dot{\theta}_{n+1,1} \cdots \dot{\theta}_{n+1,6}\right]^{\mathrm{T}}, \quad n = 3, 4, \text{ or } 5. \tag{6.50}$$

6.3.3.3 Global Velocity Equations

1. Rigid Model:
   Now, considering the parallel component of the mechanism, the parallel Jacobian matrix can be obtained by differentiating (6.37), (6.39), and (6.40) with respect to time. One has

$$\dot{\mathbf{b}}'_i = l_{i1}\mathbf{Q}_{ti1}\dot{\mathbf{d}}_i, \quad i = 1, \ldots, n, \ n = 3, 4, \text{ or } 5, \tag{6.51}$$

$$\dot{\mathbf{d}}_{i1} = \begin{bmatrix} 0 \\ -\sin\theta_{i1} \\ \cos\theta_{i1} \end{bmatrix} \dot{\theta_{i1}}, \quad i = 1, \ldots, n, \ n = 3, 4, \text{ or } 5, \tag{6.52}$$

$$(\mathbf{p}_i - \mathbf{b}'_i)^{\mathrm{T}}\dot{\mathbf{b}}'_i - (\mathbf{p}_i - \mathbf{b}'_i)^{\mathrm{T}}\dot{\mathbf{p}}_i = 0, \quad i = 1, \ldots, n, \ n = 3, 4, \text{ or } 5. \tag{6.53}$$

One obtains

$$\dot{\mathbf{p}}_i = \dot{\mathbf{p}} + \dot{\mathbf{Q}}\mathbf{r}'_i, \quad i = 1, \ldots, n, \ n = 3, 4, \text{or } 5 \tag{6.54}$$

assuming

$$\mathbf{e}_i = l_{i1}\mathbf{Q}_{ti1}\begin{bmatrix} 0 \\ -\sin\theta_{i1} \\ \cos\theta_{i1} \end{bmatrix}, \quad i = 1, \ldots, n, \ n = 3, 4, \text{or } 5 \tag{6.55}$$

then

$$\dot{\mathbf{b}}'_i = \mathbf{e}_i\dot{\theta}_{i1}, \quad i = 1, \ldots, n, \ n = 3, 4, \text{or } 5 \tag{6.56}$$

therefore (6.53) can be rewritten as (for $i = 1, \ldots, n, \quad n = 3, 4, \text{or } 5$)

$$(\mathbf{p}_i - \mathbf{b}'_i)^{\mathrm{T}}\mathbf{e}_i\dot{\theta_{i1}} = (\mathbf{p}_i - \mathbf{b}'_i)^{\mathrm{T}}\dot{\mathbf{p}} + [(\mathbf{Q}\mathbf{r}'_i) \times (\mathbf{p}_i - \mathbf{b}'_i)]^{\mathrm{T}}\omega. \tag{6.57}$$

Hence, one has the velocity equation as

$$\mathbf{A}\mathbf{t} = \mathbf{B}\dot{\theta}, \tag{6.58}$$

where vector $\dot{\theta}$ and $\mathbf{t}$ are defined as

$$\dot{\theta} = \begin{bmatrix} \dot{\theta}_1 \cdots \dot{\theta}_n \end{bmatrix}^{\mathrm{T}}, \quad n = 3, 4, \text{or } 5, \tag{6.59}$$

$$\mathbf{t} = \begin{bmatrix} \omega_1 \ \omega_2 \ \omega_3 \ \dot{x} \ \dot{y} \ \dot{z} \end{bmatrix}^{\mathrm{T}}, \tag{6.60}$$

vector $\boldsymbol{\omega}$ is the angular velocity of the platform, and

$$\mathbf{A} = \begin{bmatrix} \mathbf{a}_1^{\mathrm{T}} \\ \mathbf{a}_2^{\mathrm{T}} \\ \vdots \\ \mathbf{a}_n^{\mathrm{T}} \end{bmatrix}, \quad \mathbf{B} = \mathrm{diag}[(\mathbf{p}_1 - \mathbf{b}'_1)^{\mathrm{T}}\mathbf{e}_1, \ldots, (\mathbf{p}_n - \mathbf{b}'_n)^{\mathrm{T}}\mathbf{e}_n], \tag{6.61}$$

where $\mathbf{a}_i$ is a six-dimensional vector, which can be expressed as

$$\mathbf{a}_i = \begin{bmatrix} (\mathbf{Q}\mathbf{r}'_i) \times (\mathbf{p}_i - \mathbf{b}'_i) \\ (\mathbf{p}_i - \mathbf{b}'_i) \end{bmatrix}, \quad i = 1, \ldots, n, \ n = 3, 4, \text{or } 5. \tag{6.62}$$

2. Compliant Model:
Differentiating (6.45) and (6.46) with respect to time, one has

$$\dot{\mathbf{b}}'_i = \mathbf{Q}_{i0}\dot{\mathbf{Q}}_{i1}\mathbf{a}_{i2} + \mathbf{Q}_{i0}\mathbf{Q}_{i1}\dot{\mathbf{a}}_{i2}, \quad i = 1, \ldots, n, \ n = 3, 4, \text{or } 5, \tag{6.63}$$

$$\dot{\mathbf{a}}_{i2} = \begin{bmatrix} -l_{i1}\sin\theta_{i2} \\ l_{i1}\cos\theta_{i2} \\ 0 \end{bmatrix} \dot{\theta}_{i2}, \quad i = 1, \ldots, n, \tag{6.64}$$

$$\dot{\mathbf{Q}}_{i1} = \begin{bmatrix} -\sin\theta_{i1} & 0 & \cos\theta_{i1} \\ \cos\theta_{i1} & 0 & \sin\theta_{i1} \\ 0 & 0 & 0 \end{bmatrix} \dot{\theta_{i1}}, \quad i = 1, \ldots, n, \ n = 3, 4, \text{ or } 5. \tag{6.65}$$

For $i = 1, \ldots, n, \quad n = 3, 4$, or 5, assuming

$$\mathbf{d}_{i1} = \mathbf{Q}_{i0} \begin{bmatrix} -\sin\theta_{i1} & 0 & \cos\theta_{i1} \\ \cos\theta_{i1} & 0 & \sin\theta_{i1} \\ 0 & 0 & 0 \end{bmatrix} \mathbf{a}_{i2}, \ \mathbf{d}_{i2} = \mathbf{Q}_{i0}\mathbf{Q}_{i1} \begin{bmatrix} -l_{i1}\sin\theta_{i2} \\ l_{i1}\cos\theta_{i2} \\ 0 \end{bmatrix} \tag{6.66}$$

then one has

$$\dot{\mathbf{b}}'_i = \mathbf{d}_{i1}\dot{\theta}_{i1} + \mathbf{d}_{i2}\dot{\theta}_{i2}, \quad i = 1, \ldots, n, \ n = 3, 4, \text{ or } 5. \tag{6.67}$$

Differentiating (6.40) with respect to time, one obtains (6.53), and following a derivation similar to the one presented above for the mechanism with rigid links, for $i = 1, \ldots, n, \quad n = 3, 4$, or 5, one obtains

$$(\mathbf{p}_i - \mathbf{b}'_i)^{\mathrm{T}}(\mathbf{d}_{i1}\dot{\theta}_{i1} + \mathbf{d}_{i2}\dot{\theta}_{i2}) = (\mathbf{p}_i - \mathbf{b}'_i)^{\mathrm{T}}\dot{\mathbf{p}} + [(\mathbf{Q}\mathbf{r}'_i) \times (\mathbf{p}_i - \mathbf{b}'_i)]^{\mathrm{T}}\omega. \tag{6.68}$$

Hence one has the velocity equation as

$$\mathbf{A}\mathbf{t} = \mathbf{B}_1\dot{\theta}_1 + \mathbf{B}_2\dot{\theta}_2, \tag{6.69}$$

where vectors $\dot{\theta}_1$ and $\dot{\theta}_2$ are defined as

$$\dot{\theta}_1 = \begin{bmatrix} \dot{\theta}_{11} \cdots \dot{\theta}_{n1} \end{bmatrix}^{\mathrm{T}}, \quad n = 3, 4, \text{ or } 5, \tag{6.70}$$

$$\dot{\theta}_2 = \begin{bmatrix} \dot{\theta}_{12} \cdots \dot{\theta}_{n2} \end{bmatrix}^{\mathrm{T}}, \quad n = 3, 4, \text{ or } 5, \tag{6.71}$$

matrices $\mathbf{A}$, $\mathbf{B}_1$ and $\mathbf{B}_2$ are given as

$$\mathbf{A} = \begin{bmatrix} \mathbf{a}_1 \ \mathbf{a}_2 \ \mathbf{a}_3 \ \mathbf{a}_4 \ \mathbf{a}_5 \ \mathbf{a}_6 \end{bmatrix}^{\mathrm{T}} \tag{6.72}$$

$$\mathbf{B}_1 = \mathrm{diag}[b_{11}, \ldots, b_{n,2n-1}], \quad n = 3, 4, \text{ or } 5, \tag{6.73}$$

$$\mathbf{B}_2 = \mathrm{diag}[b_{12}, \ldots, b_{n,2n}], \quad n = 3, 4, \text{ or } 5, \tag{6.74}$$

where $\mathbf{a}_i$ is a six-dimensional vector and $\mathbf{b}_{i,2i-1}$, $\mathbf{b}_{i,2i}$ are the diagonal items of $\mathbf{B}_1$ and $\mathbf{B}_2$, respectively. They can be expressed as

$$\mathbf{a}_i = \begin{bmatrix} (\mathbf{Q}\mathbf{r'}_i) \times (\mathbf{p}_i - \mathbf{b}'_i) \\ (\mathbf{p}_i - \mathbf{b}'_i) \end{bmatrix}, \quad i = 1, \ldots, n, \ n = 3, 4, \text{or } 5, \tag{6.75}$$

$$b_{i,2i-1} = (\mathbf{p}_i - \mathbf{b}'_i)^{\mathrm{T}} \mathbf{d}_{i,1}, \quad i = 1, \ldots, n, \ n = 3, 4, \text{or } 5, \tag{6.76}$$

$$b_{i,2i} = (\mathbf{p}_i - \mathbf{b}'_i)^{\mathrm{T}} \mathbf{d}_{i,2}, \quad i = 1, \ldots, n, \ n = 3, 4, \text{or } 5. \tag{6.77}$$

6.3.4 Kinetostatic Model for the Mechanism with Rigid Links

According to the principle of virtual work, one can finally obtain the Cartesian compliance matrix with the same approach as in Chap. 5.

$$\mathbf{C}_{\mathrm{c}} = \mathbf{J}_{n+1}(\mathbf{A}\mathbf{J}_{n+1})^{-1}\mathbf{B}\mathbf{C}\mathbf{B}^{\mathrm{T}}(\mathbf{A}\mathbf{J}_{n+1})^{-\mathrm{T}}\mathbf{J}_{n+1}^{\mathrm{T}} \tag{6.78}$$

with

$$\Delta\mathbf{c} = \mathbf{C}_{\mathrm{c}}\mathbf{w}, \tag{6.79}$$

where $\mathbf{C}_{\mathrm{c}}$ is a symmetric positive semidefinite (6×6) matrix, as expected.

6.3.5 Kinetostatic Model for the Mechanism with Flexible Links

Again, based on the principle of virtual work, one can write

$$\mathbf{w}^{\mathrm{T}}\mathbf{t} = \tau_{n+1}^{\mathrm{T}}\dot{\theta}'_{n+1} + \tau_1^{\mathrm{T}}\dot{\theta}_1 + \tau_2^{\mathrm{T}}\dot{\theta}_2, \tag{6.80}$$

where τ_1 and τ_2 correspond to a partition of vector τ, in components associated with $\dot{\theta}_1$ and $\dot{\theta}_2$, respectively, i.e., the first and second joint of each leg. τ is the vector of actuator forces, $\dot{\theta}$ is the vector of actuator velocities (actuated joints and joints with virtual springs), and τ_{n+1} is the vector of joint torques in the passive constraining leg. This vector is defined as follows, where $\mathbf{K}_{n+1}$ is the stiffness matrix of the passive constraining leg,

$$\tau_{n+1} = \mathbf{K}_{n+1}\Delta\theta'_{n+1}, \tag{6.81}$$

$$\tau_1 = \mathbf{K}_{j1}\Delta\theta_1, \tag{6.82}$$

$$\tau_2 = \mathbf{K}_{j2}\Delta\theta_2, \tag{6.83}$$

$$\mathbf{K}_{j1} = \mathrm{diag}[k_{11}, \ldots, k_{n1}], \tag{6.84}$$

$$\mathbf{K}_{j2} = \mathrm{diag}[k_{12}, \ldots, k_{n2}]. \tag{6.85}$$

Matrix $\mathbf{K}_{n+1}$ is a diagonal 6×6 matrix in which the ith diagonal entry is zero if it is associated with a real joint or it is equal to k_i if it is associated with a virtual joint, where k_i is the stiffness of the virtual spring located at the ith joint. $k_{11},\ldots,k_{n1}$ are the compound stiffnesses of actuators and first links stiffnesses while $k_{12},\ldots,k_{n2}$ are the first links stiffnesses. One can rewrite (6.69) as

$$\dot{\theta}_1 = \mathbf{B}_1^{-1}\mathbf{A}\mathbf{t} - \mathbf{B}_1^{-1}\mathbf{B}_2\dot{\theta}_2. \tag{6.86}$$

Substituting (6.86) and (6.49) into (6.80), one can obtain

$$\mathbf{w}^{\mathrm{T}}\mathbf{J}'_{n+1}\dot{\theta}'_{n+1} = \tau_{n+1}^{\mathrm{T}}\dot{\theta}'_{n+1} + \tau_2^{\mathrm{T}}\dot{\theta}_2 + \tau_1^{\mathrm{T}}\mathbf{B}_1^{-1}\mathbf{A}\mathbf{J}'_{n+1}\dot{\theta}'_{n+1} - \tau_1^{\mathrm{T}}\mathbf{B}_1^{-1}\mathbf{B}_2\dot{\theta}_2. \tag{6.87}$$

Since there are 11 degrees of freedom in the compliant mechanism, this equation must be satisfied for any value of $\dot{\theta}'_{n+1}$ and $\dot{\theta}_2$. Therefore, one can equate the coefficients of the terms in $\dot{\theta}'_{n+1}$ and the terms in $\dot{\theta}_2$, hence one can obtain

$$(\mathbf{J}'_{n+1})^{\mathrm{T}}\mathbf{w} = \tau_{n+1} + (\mathbf{J}'_{n+1})^{\mathrm{T}}\mathbf{A}^{\mathrm{T}}\mathbf{B}_1^{-\mathrm{T}}\tau_1, \tag{6.88}$$

$$\tau_2 = \mathbf{B}_2^{\mathrm{T}}\mathbf{B}_1^{-\mathrm{T}}\tau_1. \tag{6.89}$$

Substituting (6.81), (6.82), and (6.83) into (6.88) and (6.89), one obtains

$$(\mathbf{J}'_{n+1})^{\mathrm{T}}\mathbf{w} = \mathbf{K}_{n+1}\Delta\theta'_{n+1} + (\mathbf{J}'_{n+1})^{\mathrm{T}}\mathbf{A}^{\mathrm{T}}\mathbf{B}_1^{-\mathrm{T}}\mathbf{K}_{j1}\Delta\theta_1, \tag{6.90}$$

$$\Delta\theta_2 = \mathbf{K}_{j2}^{-1}\mathbf{B}_2^{\mathrm{T}}\mathbf{B}_1^{-\mathrm{T}}\mathbf{K}_{j1}\Delta\theta_1. \tag{6.91}$$

Substituting (6.91) into (6.69), one obtains

$$\mathbf{A}\mathbf{t} = \mathbf{W}\dot{\theta}_1, \tag{6.92}$$

where

$$\mathbf{W} = \mathbf{B}_1 + \mathbf{B}_2\mathbf{K}_{j2}^{-1}\mathbf{B}_2^{\mathrm{T}}\mathbf{B}_1^{-\mathrm{T}}\mathbf{K}_{j1}. \tag{6.93}$$

Substituting (6.92) into (6.90), one obtains

$$(\mathbf{J}'_{n+1})^{\mathrm{T}}\mathbf{w} = \mathbf{K}_{n+1}(\mathbf{J}'_{n+1})^{-1}\Delta\mathbf{c} + (\mathbf{J}'_{n+1})^{\mathrm{T}}\mathbf{A}^{\mathrm{T}}\mathbf{B}_1^{-\mathrm{T}}\mathbf{K}_{j1}\mathbf{W}^{-1}\mathbf{A}\Delta\mathbf{c}, \tag{6.94}$$

i.e.,

$$\mathbf{w} = ((\mathbf{J}'_{n+1})^{-\mathrm{T}}\mathbf{K}_{n+1}(\mathbf{J}'_{n+1})^{-1} + \mathbf{A}^{\mathrm{T}}\mathbf{B}_1^{-\mathrm{T}}\mathbf{K}_{j1}\mathbf{W}^{-1}\mathbf{A})\Delta\mathbf{c}, \tag{6.95}$$

which is in the form

$$\mathbf{w} = \mathbf{K}\Delta\mathbf{c}, \tag{6.96}$$

where $\mathbf{K}$ is the stiffness matrix, which is equal to

$$\mathbf{K} = [(\mathbf{J}'_{n+1})^{-\mathrm{T}}\mathbf{K}_{n+1}(\mathbf{J}'_{n+1})^{-1} + \mathbf{A}^{\mathrm{T}}\mathbf{B}_1^{-\mathrm{T}}\mathbf{K}_{j1}\mathbf{W}^{-1}\mathbf{A}]. \tag{6.97}$$

Matrix $\mathbf{K}$ is a symmetric (6×6) positive semidefinite matrix, as expected. Matrix $\mathbf{K}$ will be of full rank in nonsingular configurations. Indeed, the sum of the two terms in (6.97) will span the complete space of constraint wrenches.

6.3.6 Examples

6.3.6.1 5-dof Parallel Mechanism

This mechanism is illustrated is Fig. 6.5, the compliance matrix for the mechanism with rigid links can be written as

$$\mathbf{C}_c = \mathbf{J}_6(\mathbf{A}\mathbf{J}_6)^{-1}\mathbf{B}\mathbf{C}\mathbf{B}^{\mathrm{T}}(\mathbf{A}\mathbf{J}_6)^{-\mathrm{T}}\mathbf{J}_6^{\mathrm{T}}, \tag{6.98}$$

where

$$\mathbf{C} = \mathrm{diag}[c_1, c_2, c_3, c_4, c_5] \tag{6.99}$$

with c_1, c_2, c_3, c_4 and c_5 the compliances of the actuators and $\mathbf{J}_6$ is the Jacobian matrix of the passive constraining leg in this 5-dof case. Matrices $\mathbf{A}$ and $\mathbf{B}$ are the Jacobian matrices of the structure without the passive constraining leg.

Similarly, the stiffness matrix for the mechanism with flexible links can be written as

$$\mathbf{K} = (\mathbf{J}_6')^{-\mathrm{T}}\mathbf{K}_6(\mathbf{J}_6')^{-1} + \mathbf{A}^{\mathrm{T}}\mathbf{B}_1^{-\mathrm{T}}\mathbf{K}_{j1}\mathbf{W}^{-1}\mathbf{A}, \tag{6.100}$$

where

$$\mathbf{K}_6 = \mathrm{diag}[0, k_{62}, 0, 0, 0, 0], \tag{6.101}$$

$$\mathbf{K}_{j1} = \mathrm{diag}[k_{11}, k_{21}, k_{31}, k_{41}, k_{51}], \tag{6.102}$$

$$\mathbf{K}_{j2} = \mathrm{diag}[k_{12}, k_{22}, k_{32}, k_{42}, k_{52}], \tag{6.103}$$

where k_{62} is the stiffness of the virtual joint of the passive constraining leg, and $\mathbf{J}_6'$ is the Jacobian matrix of the passive constraining leg in this 5-dof case. Matrices $\mathbf{A}$ and $\mathbf{B}$ are the Jacobian matrices of the structure without the passive constraining leg.

The comparison between the parallel mechanism with rigid links (without virtual joints) and the parallel mechanism with flexible links (with virtual joints) is given in Table 6.2.

6.3.6.2 4-dof Parallel Mechanism

This mechanism is illustrated is Fig. 6.9, the compliance matrix for the mechanism with rigid links will be

$$\mathbf{C}_{\mathrm{c}} = \mathbf{J}_5(\mathbf{A}\mathbf{J}_5)^{-1}\mathbf{B}\mathbf{C}\mathbf{B}^{\mathrm{T}}(\mathbf{A}\mathbf{J}_5)^{-\mathrm{T}}\mathbf{J}_5^{\mathrm{T}} \tag{6.104}$$

Table 6.2 Comparison of the 5-dof mechanism compliance between the mechanism with flexible links and the mechanism with rigid links

K_{actuator}	K_{link}	κ_{θ_x}	κ_{θ_y}	κ_{θ_z}	κ_x	κ_y	κ_z
1,000	1,000	0.255808	0.478997	0.766154	0.00479741	0.0116413	0.00169207
1,000	$10^1 K_a$	0.137552	0.257339	0.412528	0.00257412	0.00625667	0.000910745
1,000	$10^2 K_a$	0.125726	0.235173	0.377165	0.0023518	0.0057182	0.000832613
1,000	$10^3 K_a$	0.124543	0.232956	0.373629	0.00232956	0.00566435	0.000824799
1,000	$10^4 K_a$	0.124425	0.232734	0.373275	0.00232734	0.00565897	0.000824018
1,000	$10^5 K_a$	0.124413	0.232712	0.37324	0.00232712	0.00565843	0.00082394
1,000	$10^6 K_a$	0.124412	0.23271	0.373236	0.00232709	0.00565838	0.000823932
1,000	$10^7 K_a$	0.124412	0.23271	0.373236	0.00232709	0.00565837	0.000823931
1,000	Rigid	0.124412	0.23271	0.373236	0.00232709	0.00565837	0.000823931

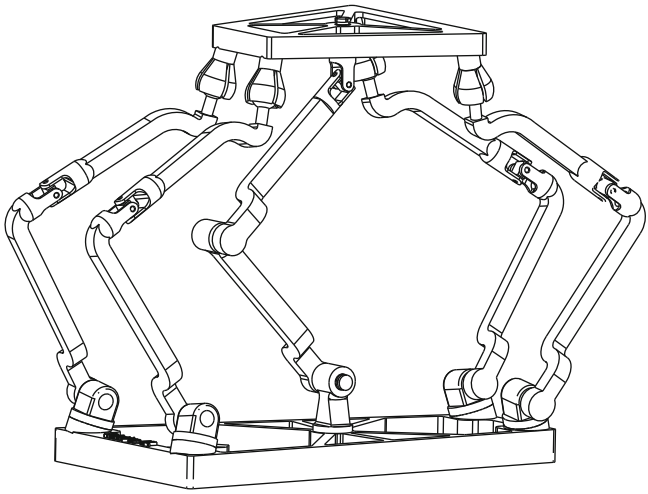

Fig. 6.9 CAD model of the spatial 4-dof parallel mechanism with revolute actuators (Figure by Gabriel Coté)

where

$$\mathbf{C} = \text{diag}[c_1, c_2, c_3, c_4] \tag{6.105}$$

with c_1, c_2, c_3, and c_4 are the compliances of the actuators and $\mathbf{J}_5$ is the Jacobian matrix of the constraining leg in this 4-dof case. Matrices $\mathbf{A}$ and $\mathbf{B}$ are the Jacobian matrices of the structure without the passive constraining leg.

Similarly, the stiffness matrix for the mechanism with flexible links can be written as

$$\mathbf{K} = (\mathbf{J}_5')^{-\mathrm{T}} \mathbf{K}_5 (\mathbf{J}_5')^{-1} + \mathbf{A}^{\mathrm{T}} \mathbf{B}_1^{-\mathrm{T}} \mathbf{K}_{j1} \mathbf{W}^{-1} \mathbf{A}, \tag{6.106}$$

Table 6.3 Comparison of the 4-dof mechanism compliance between the mechanism with flexible links and the mechanism with rigid links

K_{actuator}	K_{link}	κ_{θ_x}	κ_{θ_y}	κ_{θ_z}	κ_x	κ_y	κ_z
1,000	1,000	3.46122	0.138363	1.5×10^{-3}	0.0146575	1.32691×10^{-3}	0.000271569
1,000	$10^1 K_a$	1.49876	0.0703633	1.5×10^{-4}	0.00717397	1.32691×10^{-4}	0.000106446
1,000	$10^2 K_a$	1.30251	0.0635633	1.5×10^{-5}	0.00642561	1.32691×10^{-5}	0.0000899335
1,000	$10^3 K_a$	1.28289	0.0628833	1.5×10^{-6}	0.00635078	1.32691×10^{-6}	0.0000882822
1,000	$10^4 K_a$	1.28093	0.0628153	1.5×10^{-7}	0.0063433	1.32691×10^{-7}	0.0000881171
1,000	$10^5 K_a$	1.28073	0.0628085	1.5×10^{-8}	0.00634255	1.32691×10^{-8}	0.0000881006
1,000	$10^6 K_a$	1.28071	0.0628079	1.5×10^{-9}	0.00634247	1.32691×10^{-9}	0.000088099
1,000	$10^7 K_a$	1.28071	0.0628078	1.5×10^{-10}	0.00634246	1.32691×10^{-10}	0.0000880988
1,000	Rigid	1.28071	0.0628078	0.0	0.00634246	0.0	0.0000880988

where

$$\mathbf{K}_5 = \text{diag}[0, k_{52}, 0, k_{54}, 0, 0], \tag{6.107}$$

$$\mathbf{K}_{j1} = \text{diag}[k_{11}, k_{21}, k_{31}, k_{41}], \tag{6.108}$$

$$\mathbf{K}_{j2} = \text{diag}[k_{12}, k_{22}, k_{32}, k_{42}], \tag{6.109}$$

where k_{52} and k_{54} are the stiffnesses of the virtual joints of the passive constraining leg, $\mathbf{J}_5'$ is the Jacobian matrix of the passive constraining leg in this 4-dof case, while $\mathbf{A}$ and $\mathbf{B}_1$, $\mathbf{B}_2$ are the Jacobian matrices of the structure without the passive constraining leg.

The comparison between the parallel mechanism with rigid links (without virtual joints) and the parallel mechanism with flexible links (with virtual joints) is given in Table 6.3. Again, the effect of link flexibility is clearly demonstrated.

6.3.6.3 3-dof Parallel Mechanism

This mechanism is illustrated is Fig. 6.10, the compliance matrix for the rigid mechanism can be written as

$$\mathbf{C}_c = \mathbf{J}_4(\mathbf{A}\mathbf{J}_4)^{-1}\mathbf{B}\mathbf{C}\mathbf{B}^{\mathrm{T}}(\mathbf{A}\mathbf{J}_4)^{-\mathrm{T}}\mathbf{J}_4^{\mathrm{T}}, \tag{6.110}$$

where $\mathbf{C}_c = \text{diag}[c_1, c_2, c_3]$, with c_1, c_2 and c_3 are the compliances of the actuators and $\mathbf{J}_4$ is the Jacobian matrix of the passive constraining leg in this 3-dof case. $\mathbf{A}$ and $\mathbf{B}$ are the Jacobian matrices of the structure without the passive constraining leg.

Similarly, the stiffness matrix for the mechanism with flexible links will be written as

$$\mathbf{K} = [(\mathbf{J}_4')^{-\mathrm{T}}\mathbf{K}_4(\mathbf{J}_4')^{-1} + \mathbf{A}^{\mathrm{T}}\mathbf{B}_1^{-\mathrm{T}}\mathbf{K}_{j1}\mathbf{W}^{-1}\mathbf{A}] \tag{6.111}$$

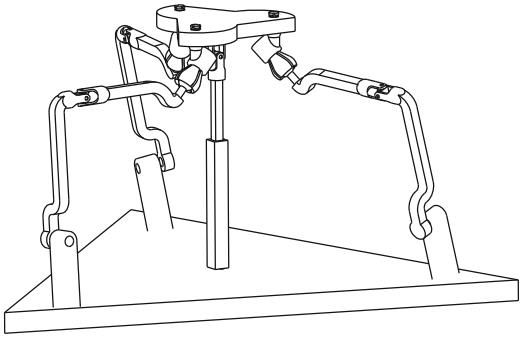

Fig. 6.10 CAD model of the spatial 3-dof parallel mechanism with revolute actuators (Figure by Gabriel Coté)

Table 6.4 Comparison of the 3-dof mechanism compliance between the mechanism with flexible links and the mechanism with rigid links

K_{actuator}	K_{link}	κ_{θ_x}	κ_{θ_y}	κ_{θ_z}	κ_x	κ_y	κ_z
1,000	1,000	0.09937	0.09937	10^{-3}	1.06152×10^{-3}	1.06152×10^{-3}	0.000186579
1,000	$10^1 K_a$	0.02904	0.02904	10^{-4}	1.06152×10^{-4}	1.06152×10^{-4}	0.0000975989
1,000	$10^2 K_a$	0.02201	0.02201	10^{-5}	1.06152×10^{-5}	1.06152×10^{-5}	0.0000887009
1,000	$10^3 K_a$	0.02131	0.02131	10^{-6}	1.06152×10^{-6}	1.06152×10^{-6}	0.0000878111
1,000	$10^4 K_a$	0.02123	0.02123	10^{-7}	1.06152×10^{-7}	1.06152×10^{-7}	0.0000877221
1,000	$10^5 K_a$	0.02123	0.02123	10^{-8}	1.06152×10^{-8}	1.06152×10^{-8}	0.0000877132
1,000	$10^6 K_a$	0.02123	0.02123	10^{-9}	1.06152×10^{-9}	1.06152×10^{-9}	0.0000877123
1,000	$10^7 K_a$	0.02123	0.02123	10^{-10}	1.06152×10^{-10}	1.06152×10^{-10}	0.0000877122
1,000	Rigid	0.02123	0.02123	0.0	0.0	0.0	0.0000877122

where $\mathbf{W}$ is defined in (6.93) and

$$\mathbf{K}_4 = \text{diag}[k_{41}, k_{42}, k_{43}, 0, 0, 0], \tag{6.112}$$

$$\mathbf{K}_{j1} = \text{diag}[k_{11}, k_{21}, k_{31}], \tag{6.113}$$

$$\mathbf{K}_{j2} = \text{diag}[k_{12}, k_{22}, k_{32}] \tag{6.114}$$

and $\mathbf{J}_4'$ is the Jacobian matrix of the passive constraining leg with virtual joints.

The comparison between the parallel mechanism with rigid links (without virtual joints) and the parallel mechanism with flexible links (with virtual joints) is given in Table 6.4. The Cartesian compliance in each of the directions is given for a reference configuration of the mechanism, for progressively increasing values of the link stiffnesses.

From Table 6.4, one can find that with the improvement of link stiffness, the mechanism's compliance with flexible links is very close to that of mechanism with rigid links. This means that one can assume the flexible mechanism to be rigid only if the link stiffness reaches a high value.

6.4 Conclusions

In this chapter, mechanisms with revolute actuators (whose degrees of freedom are 3, 4, 5 and 6) have been considered. Solutions for the inverse kinematic problem have been given. The Jacobian matrices obtained have been used to establish the kinetostatic model of the mechanisms. The lumped models of the link and joint compliances have been used for the study of the Cartesian compliance. It has been shown that the kinetostatic analysis can be used to assess the stiffness properties of this family of mechanisms. Finally, examples have been investigated and numerical results have been obtained and the results clearly demonstrate the relevance of the kinetostatic analysis in the context of design of such mechanisms.